Growth and Optical Properties of SrBi₂Nb₂O₉ Ferroelectric Thin Films Using Pulsed Laser Deposition

Pingxiong Yang

David L. Carroll

John Ballato

Robert W. Schwartz
Missouri University of Science and Technology

Growth and optical properties of $SrBi_2Nb_2O_9$ ferroelectric thin films using pulsed laser deposition

Pingxiong Yang,[a] David L. Carroll, and John Ballato
Center for Optical Materials Science and Engineering Technologies, School of Materials Science and Engineering, Clemson University, Clemson, South Carolina 29634-0971

Robert W. Schwartz
Department of Ceramic Engineering, University of Missouri, Rolla, Missouri 65409-0330

High quality $SrBi_2Nb_2O_9$ ferroelectric thin films were fabricated on platinized silicon using pulsed laser deposition assisted with dc glow discharge plasma. Microstructure and ferroelectric properties of the films were characterized. Optical properties of the thin films were studied by spectroscopic ellipsometry and photoluminescence from the ultraviolet to the infrared region. Optical constants, $n \sim 0.56$ in the infrared region and $n \sim 2.24$ in the visible spectral region, were determined through multilayer analyses on their respective pseudodielectric functions. The band-gap energy is estimated to be 3.60 eV. A photoluminescence peak at 0.78 μm, whose intensity decreases with decreasing temperature, was observed when excited with subband-gap energy (2.41 eV). This emission process may involve intermediate defect states at the crystallite boundaries. A possible mechanism for the observed photoluminescence, a $Nb^{4+}-O^-$ exciton in the NbO_6 octahedron, is discussed. © *2003 American Institute of Physics.* [DOI: 10.1063/1.1571219]

I. INTRODUCTION

Ferroelectric thin films of layered perovskite compositions have attracted great attention.[1-9] These materials, especially $SrBi_2Ta_2O_9$ (SBT), are key candidates for nonvolatile memory devices because they possess excellent fatigue resistance and electrical properties, even when film thickness is reduced to under 200 nm thickness.[5] These exceptional properties are retained even when simple Pt electrodes are utilized. Recently, investigation of the optical properties of these materials has become an area of increasing interest due to applications in uncooled infrared detectors,[10,11] optical sensor protection,[12] and waveguides.[13,14] The general chemical formula of this family is $(Bi_2O_2)^{2+}(A_{m-1}B_mO_{3m+1})^{2-}$, where A (a divalent metal such as Sr, Ba, Ca, Pb) and B (a metal of valence 5+, usually, Ta or Nb) are standard A-site and B-site cations which center in the perovskite structure, and m is the number of perovskite unit cells between (Bi_2O_2) layers. The size of the A-site cation influences the structural distortion due to increasing lattice mismatch between AO and BO_2 planes, which causes changes in the properties.[15,16] Similarly, Nb substitution for Ta also causes some structural distortions leading to changes in material properties. Additional reports suggest that other layered perovskite materials may possess properties that are even more attractive than $SrBi_2Ta_2O_9$.[17] It is therefore desirable to study the synthesis and properties of other Aurivillius compounds, such as $SrBi_2Nb_2O_9$ (SBN).

Compared with other techniques utilized for thin film deposition, the key advantage of pulsed laser deposition (PLD) is compositional fidelity between the target and deposited film, which is important to obtain high quality multicomponent thin films. In order to offer low temperature processing, to minimize a chemical reaction between the film and substrate, and to control the stoichiometry and structure of the film, the introduction of a low pressure dc glow discharge during laser deposition is believed to be beneficial. This technique has been reported for high T_c superconducting and ferroelectric $Pb(Zr,Ti)O_3$ (PZT) thin films.[18-20] Therefore it is worth exploring this technique for growing high quality SBN ferroelectric thin films.

In this article, we report on the synthesis of SBN ferroelectric thin films prepared by pulsed laser deposition (PLD) with dc glow discharge and optical properties of the films from the infrared to ultraviolet regions, as determined by spectroscopic ellipsometry (SE) and photoluminescence (PL).

II. EXPERIMENT

The samples were fabricated on platinized silicon ($Pt/Ti/SiO_2/Si$) using PLD assisted by a dc glow discharge plasma. The laser used for SBN thin film deposition was an XeCl (Lambda Physik LPX220icc, wavelength 308 nm) excimer laser with 5 Hz repetition frequency, 17 ns pulse duration, and an energy of 160 mJ/pulse. The output laser beam was focused onto a rotating target at an angle of 45° by a UV lens with a focal length of 50 cm. The stability of the incoming beam was monitored using an energy meter. In order to take advantage of low temperature processing,[20] in order to minimize the chemical reaction between the film and substrate and control stoichiometry and structure, a low oxygen pressure dc glow discharge was used during laser deposition. A copper ring was placed halfway between the target and substrate. The substrate and target were electrically grounded while the ring was held at 700 V.
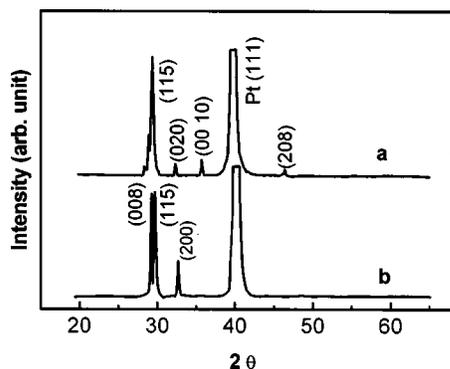
[a]Electronic mail: pxyang@clemson.edu

FIG. 1. XRD pattern for SBN films. (a) Without and (b) with the dc glow discharge assist.

The SBN target was processed by mixing $SrCO_3$, Bi_2O_3, and Nb_2O_5 powders in a stoichiometric ratio using ball milling, followed by calcination of the mixed powders at 940 °C. The calcined powders were then pressed at 800 kg/cm² in a circular die and the pressed pellets were sintered at 1200 °C for 2 h in a regular box furnace. The target was freshly polished to produce a uniform plasma cloud and mounted on a motor-driven rotary shaft.

The platinized silicon $(Pt/Ti/SiO_2/Si)$ substrates were prepared from wafers of (111) oriented Si with a layer of thermally grown SiO_2, then coated with 10 nm Ti and 800 nm Pt using a UHV electron beam evaporator (Balzers UMS500p) and Ti and Pt targets, respectively. The substrates, whose temperatures were at 400 °C during deposition, were mounted onto a heated substrate holder and placed parallel to the target at a distance of 4 to 5 cm.

Before deposition, the chamber was initially pumped down to 5 Pa by a mechanical pump, and high purity oxygen was then introduced using a mass flow controller at a flow rate of 20 cm³/min, until an approximate pressure of 20 Pa was obtained. The films were deposited on the platinized silicon substrates at 400 °C and annealed at 750 °C for 90 min in oxygen.

The crystallographic structure of the SBN films was characterized by x-ray diffraction (XRD) using Cu $K\alpha$ radiation. The microstructure of the films was observed by transmission electron microscopy (TEM). The ferroelectric behavior and fatigue endurance were investigated using a RT66A (Radiant Technologies). The optical properties of the films were measured using photoluminescence (PL) and spectroscopic ellipsometery (SE). The SE measurements were carried out at room temperature using two automatic spectroscopic ellipsometers in the 2–16 μm (infrared) and 0.24–0.85 μm (ultraviolet) ranges, respectively.[21,22] The PL measurements were performed from liquid-helium to room temperature on a Nicolet 800 Fourier transform spectrometer, using an Ar-ion (0.5145 μm) laser for excitation.

III. RESULTS AND DISCUSSION

A. Microstructure

The crystallographic structure of SBN films was characterized by x-ray diffraction (XRD) using Cu $K\alpha$ radiation
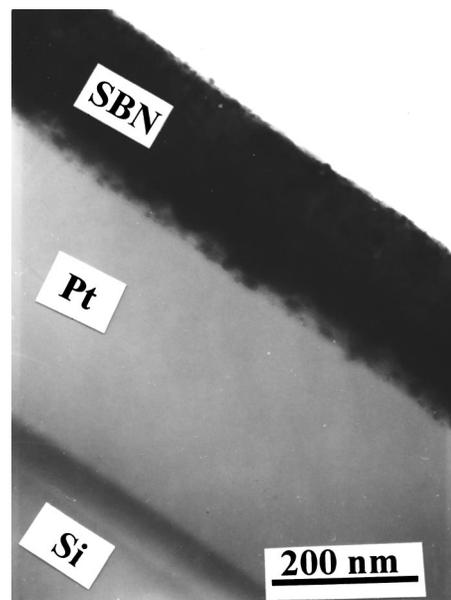

FIG. 2. Cross-section TEM micrograph of a typical SBN film.

and the results are shown in Fig. 1. The XRD pattern shows that the dominant orientations of the films on platinized silicon are (008), (200), and (115). Compared with our previous work without the dc glow discharge assist,[23] the films have an additional strong (008). This is due to the discharge plasma and the electrical poling of the 700 V bias field. The introduction of a low pressure dc glow discharge has been reported for $Pb(Zr,Ti)O_3$ (PZT) ferroelectric thin films to enhance the formation of the perovskite phase, improve the electrical behavior, and increase the c-axis orientation of the films.[19,20] During film growth using laser ablation, the role of the discharge plasma can be imagined in terms of enhancing the reaction rate and modifying the growth kinetics. A dc discharge produces a flux of predominately O_2^+, and O^+ ions. In this experiment, the substrate was grounded electrically; O_2^+ and O^+ ions arrive at the substrate surface and react with the incumbent Bi atoms, increasing the probability of Bi incorporation into the film. Similarly, the grounding target electrically had limited Bi deviation at the target surface effectively. Thus as the Bi-deficient pyrochlore phase[24] was reduced, the quality of the films was improved.

A cross-section TEM micrograph of the films is shown in Fig. 2. The interface between the film and substrates is very abrupt, and the film is very dense. The observed microstructure density may be the result of modifying the growth kinetics by the discharge plasma. The large average kinetic energy of the depositing species inherent in pulsed laser deposition and high density target also likely contribute to the dense microstructure. The film thickness is about 200 nm. Moreover, the SBN film exhibits a columnar structure, indicating that the grain growth process is dictated by nucleation at the substrate surface. This is an expected result for films prepared by the physical vapor deposition processes.

In order to examine the quality of the thin films further, the ferroelectric characteristics were measured. The samples for ferroelectric property investigation were typical sandwich structure Pt/SBN/Pt capacitor devices and a representative
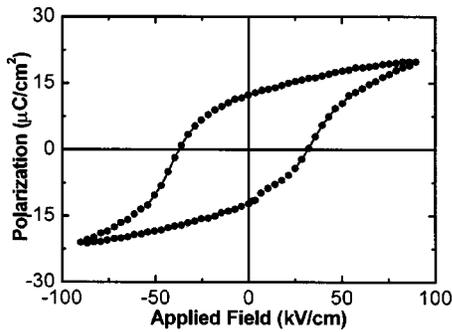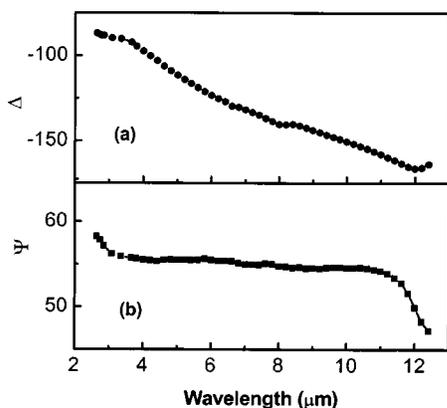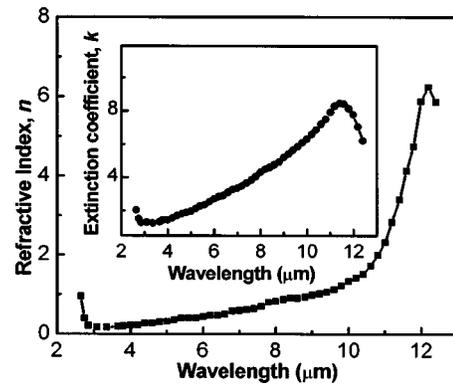
FIG. 3. Polarization–electric field hysteresis loop of an SBN thin film.

FIG. 5. Multilayer analysis of refractive index n and extinction coefficient k (inset) for the infrared region for a $SrBi_2Nb_2O_9$ film.

hysteresis loop is shown in Fig. 3. The remanent polarization (P_r) and coercive field (E_c) are approximately 11.46 $\mu C/cm^2$ and 34.86 kV/cm, respectively. These values are typical of SBN films that have been prepared previously by PLD.[7,23] A 1 kHz bipolar square wave with a magnitude of 3 V was used to fatigue the films. Excellent fatigue resistance was observed; the P_r during 10^{10} switching cycles did not show significant reduction.

B. Optical properties

The optical constants of the films are derived from SE measurements that were carried out at room temperature using ellipsometers with variable-angle, synchronously rotating polarizers and analyzers. The measured Δ and Ψ spectra for the SBN films on Pt/Ti/SiO$_2$/Si substrates in the infrared region are shown in Figs. 4(a) and 4(b), respectively. In order to estimate the optical constants of the SBN films, the ellipsometric spectra were analyzed by multilayer modeling[25] a three-layer (air, SBN film, and Pt substrate) system. In the three-layer system, the platinum layer is sufficiently thick that the incident light could not propagate through it, so the platinized silicon substrate (including the thermal oxide and the Ti adhesion layer) can be treated as a single Pt layer. The optical constants of the Pt layer come from SE measurement on a platinum film. The unknown optical constants of the SBN film were constructed by employing the modified classical dispersion relation from previous work, which is usu-

ally used to describe the dielectric function of the induced polarization.[11] The complex dielectric function $\epsilon = \epsilon' + i\epsilon''$ for N cells per unit volume is given by

$$\epsilon = \epsilon_\infty - \frac{NQ^2}{M^*\epsilon_0} \frac{\eta^2 - i\,\eta/\upsilon}{1 + \upsilon^2\eta^2}, \tag{1}$$

where ϵ_∞ and ϵ_0 are the high-frequency dielectric constant and the vacuum dielectric constant, respectively, Q is the ionic average effective charge, M^* is the reduced mass of the cations and anions in a unit cell, υ is the incident light frequency, and η is an energy-independent relaxation time. The optical constants of the SBN films were determined by fitting the model function to the measured data. A root-mean-square fractional error (σ)[11] was employed to judge the quality of the fit and to calibrate parameters. The estimated film thickness of 199.6 ± 2.1 nm from the fitting is in good agreement with the measured value obtained by TEM, as shown in Fig. 2.

The optical constants n and k in the infrared region for the SBN film are shown in Fig. 5. With increasing wavelength incident light, the refractive index and extinction coefficient first decrease, followed by a wide flat response, then quickly increase and arrive at a maximum value, before finally again decreasing. This response is typical of that of dielectric materials. As shown in Fig. 5, the refractive index of the SBN film in the reflection region (3–10 μm) is about 0.56 at 7.0 μm, while the peak value in the absorption region is about 6.24 at 12.2 μm. Like SBT films,[10] the peak in Fig. 5 results from the intrinsic vibration absorption. It is also worth noting that Δ in the infrared region is negative (Fig. 4), which indicates the dielectric constant for SBN is also negative, as observed previously for SBT films.[10] The anomalous negative dielectric constant implies that the attenuation of light propagating in the film results from scattering, not from absorption.[26] The origin of scattering may be from ferroelectric domain walls.[12]

Figures 6(a) and 6(b) show the measured Δ and Ψ spectra in the ultraviolet-visible range for the SBN films on Pt/Ti/SiO$_2$/Si substrates. For this spectral range, the optical constants for the films are mainly contributed to the direct band-gap (E_g) transition. Thus a parametric dielectric function model, which has been discussed by Adachi,[27] is em-
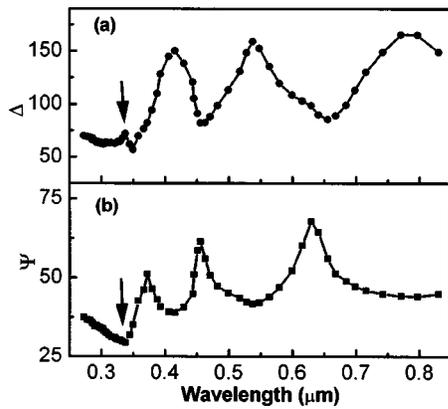

FIG. 4. (a) Δ and (b) Ψ values in the infrared region for a $SrBi_2Nb_2O_9$ film grown on platinized silicon.

FIG. 6. (a) Δ and (b) Ψ values in the ultraviolet-visible range for a SrBi$_2$Nb$_2$O$_9$ film grown on platinized silicon. The arrow indicates the band-gap energy.

FIG. 8. Optical absorption spectra of SrBi$_2$Nb$_2$O$_9$ film on MgO substrate.

ployed to construct the unknown optical constants of the SBN film, giving the dielectric function ϵ as a function of photon energy as

$$\epsilon(E) = \chi_0 (2\sqrt{E_g} - \sqrt{E_g - E - i\zeta} - \sqrt{E_g + E + i\zeta}), \quad (2)$$

where χ_0, E_g, and ζ are the amplitude, transition energy, and damping parameter, respectively, and E is the photon energy. The optical constants of SBN film in the region were determined by fitting the model function to the measured data. The estimated film thickness of 198.8 ± 1.2 nm from the fitting is also in good agreement with the measured values by TEM (Fig. 2).

The optical constants n and k of the SBN film in the ultraviolet-visible range are displayed in Fig. 7. In the visible range, the refractive index of the SBN film is about 2.24 at 0.60 μm, with an extinction coefficient of 0.001 at 0.60 μm. In the ultraviolet range, however, a peak of the refractive index in Fig. 7 appears at 0.345 μm (3.60 eV), which likely corresponds to the direct-band-gap energy E_g transition. The E_g energy is indicated by arrows in Figs. 6(a) and 6(b). It may be seen that the E_g energy corresponds to a peak value in Δ appearing at the beginning of the interference oscillations.

Optical absorption spectra of SBN thin film is presented in Fig. 8. A absorption cliff appeared between 0.30 and 0.37
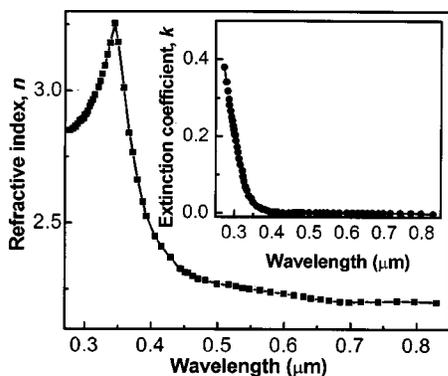
μm in the spectra, which results from the direct-band-gap energy E_g of SBN thin film absorption. The absorption edge was observed at around 0.347 μm ($\sim$3.6 eV) in Fig. 8. The result of optical absorption spectra is in very good agreement with the spectroscopic ellipsometry.

The 3.60 eV band gap for SBN is narrower than the band gap of stoichiometric SBT films (4.1 eV),[28] but the polarization (11.46 μC/cm^2 in Fig. 3) and n ($\sim$2.24 in Fig. 7) for the SBN film are greater than the corresponding values (10.0 μC/cm^2 and $n \sim 2.0$)[3,6] of SBT. In the transparent region, the dielectric constant, which is related to the polarization, is $\epsilon \sim n^2$. Therefore the higher remanent polarization values noted for SBN compared to SBT suggest a higher n value for SBN than should be observed, which is in agreement with our experimental observations. The decrease in direct-band-gap energy with increasing refractive index in these layered perovskite systems is a good agreement with empirical observations on II–VI and III–V group semiconductors.[29,30] Compared to SBT, in SBN films, due to the reduced extension of the Nb $4d$ orbital than the Ta $5d$ orbital, the hybridization of the Nb $4d$ orbital with the O $2p$ orbital increases bonding energy, resulting in a bond with greater covalent character. The greater covalent interaction of the bonds in the octahedral unit enhances the structural distortion and leads to the changes in the properties such as polarization, refractive index, and band gap.[31,32]

Finally, PL at various temperatures for the SBN films of the present study is shown in Fig. 9. As illustrated, a peak is observed at 0.78 μm (1.59 eV), and its intensity increases with increasing temperature. In this experiment, the SBN

FIG. 7. Multilayer analysis of refractive index n and extinction coefficient k (inset) in the ultraviolet-visible range for a SrBi$_2$Nb$_2$O$_9$ film.
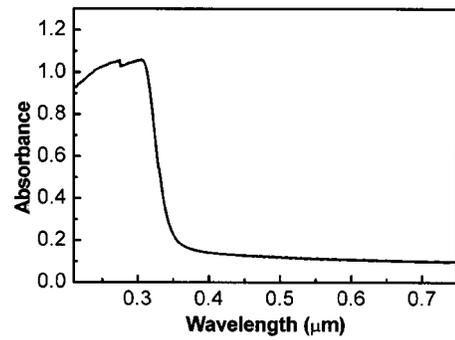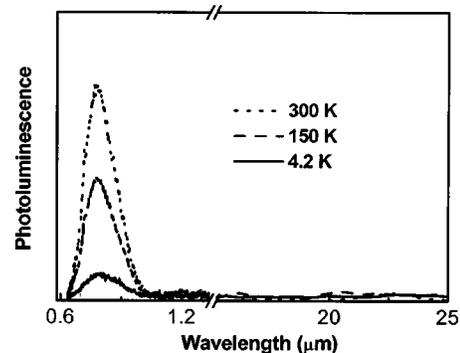

FIG. 9. Photoluminescence spectra of SrBi$_2$Nb$_2$O$_9$ films as a function of temperature.

sample for PL was excited with radiation energy (2.41 eV) smaller than the band gap (3.60 eV from the above measurement). For the subband-gap 2.41 eV light, the PL process may involve intermediate defect states at the crystallite boundaries. The origin of the luminescence band has been discussed in terms of several mechanisms for related Ti- or Ta-containing perovskites.[33–35] The paper by Li *et al.* suggests it is a defect-bound or self-trapped exciton, for example, $Ta^{4+}-O^-$ in a TaO_6 octahedron for SBT film.[34] Based on this previous assignment, we believe that the origin of the PL for our SBN film arises from the $Nb^{4+}-O^-$ exciton. Calculations suggest that the electron traps at B^{5+} ions, or B^{4+} centers in the layered perovskite system, and these B^{4+} levels are shallow (~ 0.2 eV) at room temperature.[36] When the temperature is decreased, however, electron trapping at the Nb^{4+} center is enhanced due to deepening of the potential well at lower temperature. In this case, the number of Nb^{5+} and/or O^{2+} ions available for the formation of $Nb^{4+}-O^-$ excitons is reduced, resulting in the decrease of PL with decreasing temperature, as observed in Fig. 9.

IV. CONCLUSIONS

High quality $SrBi_2Nb_2O_9$ (SBN) ferroelectric thin films have been fabricated on platinized silicon using plasma assisted PLD. The crystallographic structure of the SBN films was characterized by x-ray diffraction and the most pronounced diffraction peaks were associated with the (008), (200), and (115) reflections. The microstructure of the films was characterized by transmission electron microscopy, and a thickness of about 200 nm, dense structure, and abrupt interface were observed. Optical constants, $n \sim 0.56$ in the infrared region and $n \sim 2.24$ in the visible light, were determined through multilayer analyses on their pseudodielectric functions, respectively. The band-gap energy was determined to be 3.60 eV. A peak at 0.78 μm, whose intensity decreases with decreasing temperature, was exhibited in photoluminescence with radiation energy (2.41 eV) smaller than the band gap. For the subband-gap 2.41 eV light, the process may involve intermediate defect states at the crystallite boundaries. A possible mechanism for the observed photoluminescence, a $Nb^{4+}-O^-$ exciton in the NbO_6 octahedron, is suggested.

[1] J. F. Scott and C. A. Araujo, Science **246**, 1400 (1989).
[2] O. Auciello, J. F. Scott, and R. Ramesh, Phys. Today **51**, 22 (1998).
[3] P. Yang, N. Zhou, L. Zheng, H. Lu, and C. Lin, J. Phys. D **30**, 527 (1997).
[4] D. Dimos, N. Al-Shareef, W. L. Warren, and B. A. Tuttle, J. Appl. Phys. **80**, 1682 (1996).
[5] C. A. P. de Araujo, J. D. Cuchiare, L. D. McMillan, M. C. Scott, and J. F. Scott, Nature (London) **374**, 627 (1995).
[6] J. Bahng, M. Lee, H. L. Park, W. Kim, J. Jeong, and K. Kim, Appl. Phys. Lett. **79**, 1664 (2001).
[7] S. B. Desu and D. P. Vijay, Mater. Sci. Eng., B **32**, 83 (1995).
[8] S. Kim, D. J. Kim, J.-P. Maria, A. I. Kingon, S. K. Streiffer, J. Im, O. Auciello, and A. R. Krauss, Appl. Phys. Lett. **76**, 496 (2000).
[9] H. N. Al-Shareef, D. Dimos, T. J. Boyle, W. L. Warren, and B. A. Tuttle, Appl. Phys. Lett. **68**, 690 (1996).
[10] Z. Huang, P. Yang, Y. Chang, and J. Chu, J. Appl. Phys. **86**, 1771 (1999).
[11] Z. Huang, X. Meng, P. Yang, Z. Zhang, and J. Chu, Appl. Phys. Lett. **76**, 3980 (2000).
[12] P. Yang, J. Xu, J. Ballato, R. Schwartz, and D. Carroll, Appl. Phys. Lett. **80**, 3394 (2002).
[13] A. Petraru, J. Schubert, M. Schmid, and C. Buchal, Appl. Phys. Lett. **81**, 1375 (2002).
[14] B. H. Park, Y. Gim, Y. Fan, Q. X. Jia, and P. Lu, Appl. Phys. Lett. **77**, 2587 (2000).
[15] Y. Shimakawa, Y. Kubo, Y. Nakagawa, T. Kamiyama, H. Asano, and F. Izumi, Appl. Phys. Lett. **74**, 1904 (1999).
[16] Y. Shimakawa, Y. Kubo, Y. Nakagawa, S. Goto, T. Kamiyama, H. Asano, and F. Izumi, Phys. Rev. B **61**, 6559 (2000).
[17] K. Watanabe, M. Tanaka, E. Sumitomo, K. Katori, H. Yagi, and J. F. Scott, Appl. Phys. Lett. **73**, 126 (1998).
[18] R. K. Singh, J. Narayan, A. K. Singh, and J. Krishnaswamy, Appl. Phys. Lett. **54**, 2271 (1989).
[19] D. Roy, S. B. Krupanidhi, and J. P. Dougherty, J. Vac. Sci. Technol. A **10**, 1927 (1992).
[20] L. Zheng, X. Hu, P. Yang, W. Xu, and C. Lin, J. Mater. Res. **12**, 1179 (1997).
[21] Z. Huang, S. Jin, S. Chen, G. Shi, L. Chen, and J. Chu, Chin. J. Infrared Millim. Waves **17**, 321 (1998).
[22] D. E. Aspnes and A. A. Studna, Appl. Opt. **14**, 220 (1975).
[23] P. Yang, C. Lin, H. Deng, and L. Zheng, J. Mater. Sci. Lett. **16**, 1856 (1997).
[24] M. A. Rodriguez, T. J. Boyle, B. A. Hernandez, C. D. Buchheit, and M. O. Eatough, J. Mater. Res. **11**, 2282 (1996).
[25] R. M. A. Azzam and N. M. Bashara, *Ellipsometry and Polarized Light* (North-Holland, Amsterdam, 1977).
[26] D. Mo, *Solid Optics* (Chinese Advanced Education Press, 1996).
[27] S. Adachi, Phys. Rev. B **35**, 7454 (1987).
[28] B. M. Melnick, J. Abrokwah, J. Hallmark, and B. Ooms, Integr. Ferroelectr. **15**, 221 (1997).
[29] T. Suzuki, H. Yaguchi, H. Okumura, Y. Ishida, and S. Yoshida, Jpn. J. Appl. Phys., Part 2 **39**, L497 (2000).
[30] P. Chen, J. E. Nicholls, M. O'Neill, J. H. C. Hogg, B. Lunn, D. E. Ashenford, M. Fay, and A. G. Cullis, Semicond. Sci. Technol. **13**, 1439 (1998).
[31] Y. Shimakawa, Y. Kubo, Y. Tauchi, T. Kamiyama, H. Asano, and F. Izumi, Appl. Phys. Lett. **77**, 2749 (2000).
[32] R. E. Cohen, Nature (London) **358**, 136 (1992).
[33] V. S. Vikhnin and S. Kapphan, Phys. Solid State **40**, 834 (1998).
[34] B. Li, F. Koch, and L. Chu, Appl. Phys. Lett. **78**, 1107 (2001).
[35] J. Meng, Y. Huang, W. Zhang, Z. Du, Z. Zhu, and G. Zou, Phys. Lett. A **205**, 72 (1995).
[36] J. Robertson, C. W. Chen, W. L. Warren, and C. D. Gutleben, Appl. Phys. Lett. **69**, 1704 (1996).